Supplementary Information for "Influence of composition-dependent thermal conductivity on the long-term evolution of primordial reservoirs in Earth's lower mantle"

Yang Li, State Key Laboratory of Lithospheric Evolution, Institute of Geology and Geophysics, Institutions of Earth Science, Chinese Academy of Sciences, Beijing, yli@mail.iggcas.ac.cn

Frédéric Deschamps, Institute of Earth Sciences, Academia Sinica, Taipei, frederic@earth.sinica.edu.tw

Zhidong Shi, State Key Laboratory of Lithospheric Evolution, Institute of Geology and Geophysics, Institutions of Earth Science, Chinese Academy of Sciences, Beijing, shizhidong19@mails.ucas.ac.cn

Joshua M. Guerrero, Institute of Earth Sciences, Academia Sinica, Taipei, joshua@earth.sinica.edu.tw

Wen-Pin Hsieh, Institute of Earth Sciences, Academia Sinica, Taipei, ironck13@gmail.com

Liang Zhao, State Key Laboratory of Lithospheric Evolution, Institute of Geology and Geophysics, Institutions of Earth Science, Chinese Academy of Sciences, Beijing, zhaoliang@mail.iggcas.ac.cn

Paul J. Tackley, Institute of Geophysics, Department of Earth Sciences, ETH Zürich, Zürich, paul.tackley@erdw.ethz.ch

Indicate the corresponding author

Correspondence to: Yang Li or Frédéric Deschamps

Contents of this file

Figures S1, S2 and S3.

Table S1

Introduction

This supplementary information file provides the parameters of the numerical models (Table S1), 1-D profiles of non-dimensional reference temperature, density, thermal expansion, and thermal conductivity (Figure S1), snapshots of initial temperature and composition fields (Figure S2), and 1-D profiles of viscosity of the models at the end of the experiments in this study (Figure S3).

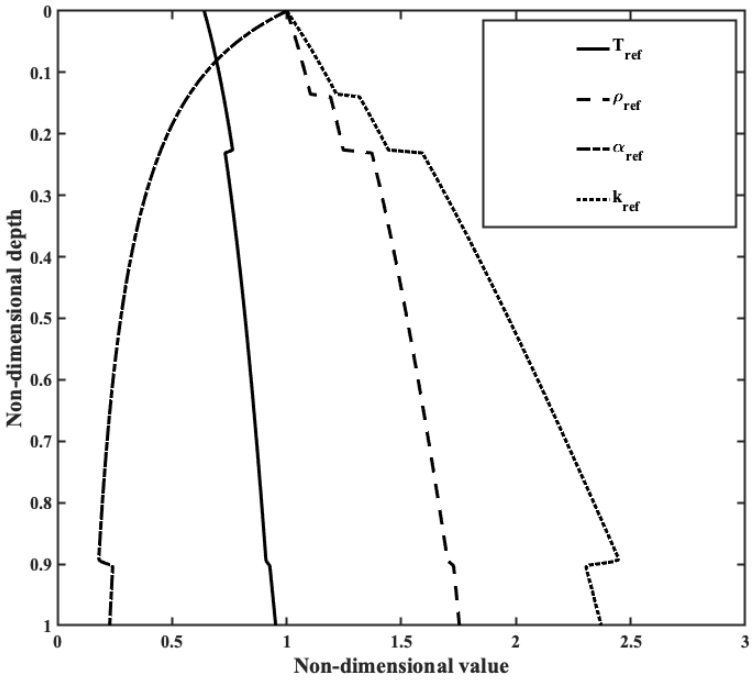

Figure S1. 1-D profiles of non-dimensional reference temperature, density, thermal expansion, and thermal conductivity (the dimensional unit can be found in Table S1).

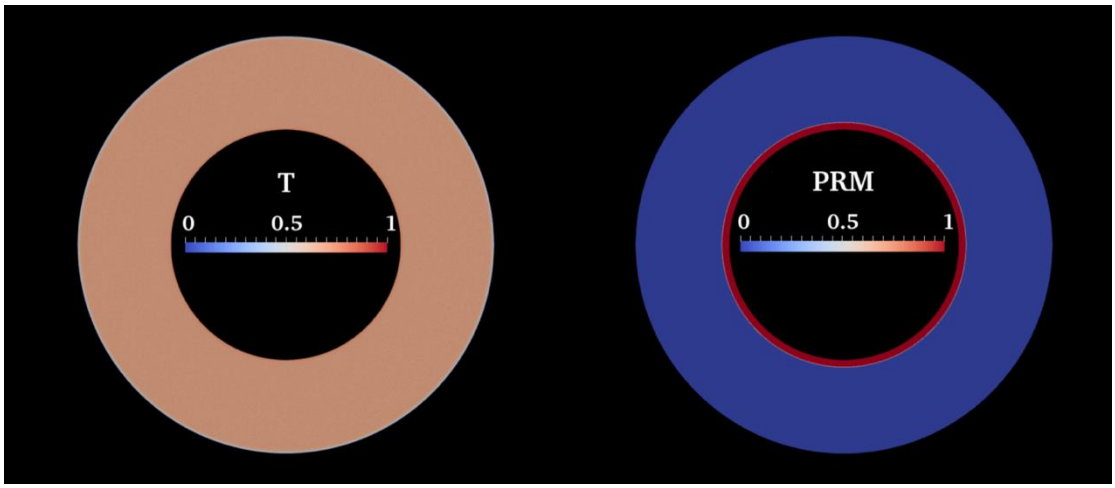

Figure S2. Snapshots of initial temperature field (left) and composition field (right).

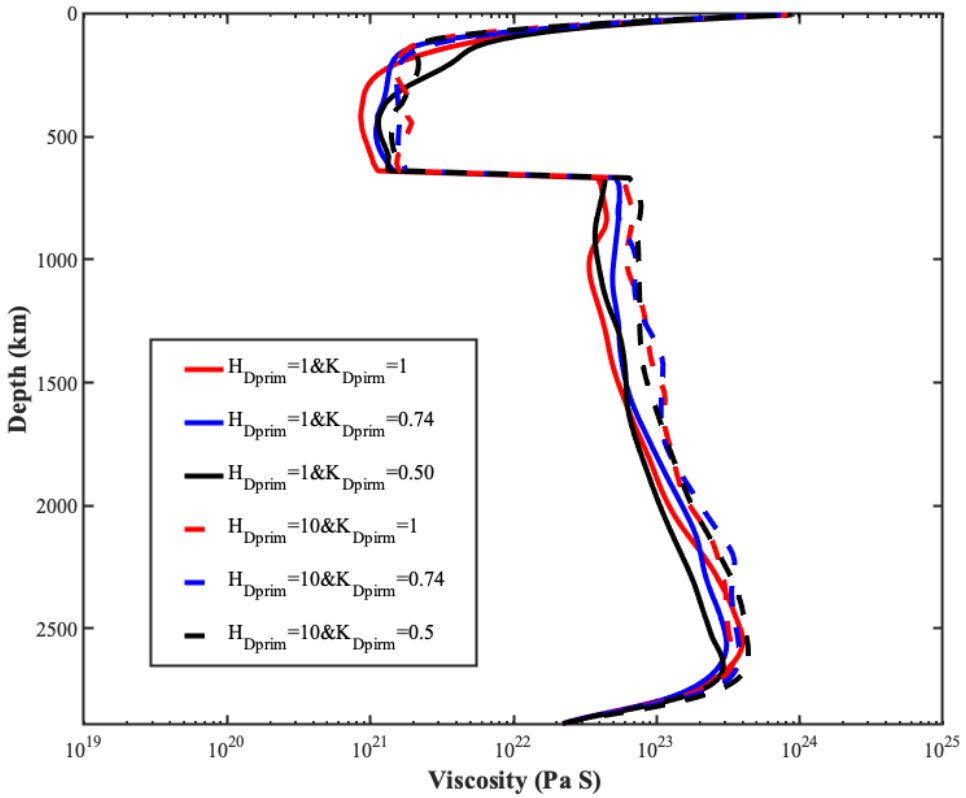

Figure S3. 1-D profiles of viscosity of the models at the end of the experiments in this study.

Table S1. Parameters of the numerical models

Parameter	Symbol	Value
Acceleration of gravity	g	9.81 m s-2
Mantle thickness	D	2891 km
Super-adiabatic temperature difference	ΔT_s	2500 K
Surface density	ρ_s	3300 kg m^{-3}
CMB density	ρ_b	5610 kg m^{-3}
Surface thermal expansion	α_s	5.0×10^{-5} K^{-1}
Surface thermal diffusivity	κ_s	7.5×10^{-7} m^2 s^{-1}
Surface thermal conductivity	k_s	3.0 W m^{-1} K^{-1}
Reference viscosity	η_0	1.96×10^{21} Pa s
Non-dimensional activation energy	E_a	20.723
Non-dimensional activation volume	V_a	4.6
Clapeyron slope at z=660km	Γ_{660}	-2.5 MPa K^{-1}
Density contrast at z=660 km	$\Delta\rho_{660}$	400 kg/m^3
Viscosity ratio at z=660km	η_{660}	30
Post-perovskite Clapeyron slope	Γ_{pPv}	13 MPa K^{-1}
Post-perovskite density contrast	$\Delta\rho_{pPv}$	62 kg/m^3
Reference internal heating rate	Rh_{ref}	4.0×10^{-12} W kg^{-1}
Surface yield stress	σ_0	200 MPa
Pressure gradient of the yield stress	σ_i	2.5×10^{-3} Pa/Pa